Bulletin of the Seismological Society of America, Vol. 71, No. 6, pp. 1719–1729, December 1981

PROCEDURES FOR COMPUTING FOCAL MECHANISMS FROM LOCAL $(SV/P)_z$ DATA

BY CARL KISSLINGER, J. ROGER BOWMAN, AND KARL KOCH

ABSTRACT

A procedure for calculating the focal mechanism of an earthquake from the distribution of the ratio of the amplitudes of *SV* to *P* waves has been developed and tested. The input consists of information taken from the hypocenter solution for the earthquake, a factor for each station that corrects for the effect of the free surface on the observed wave amplitudes and the observed values of the ratio of the vertical component of *P* to the vertical component of *SV*. The procedure starts with the selection of a slip direction. The program then finds the best fault strike and dip corresponding to that slip direction, with "best" measured by the smallest scatter of the dip for any strike. All three fault parameters are then adjusted by an iterative least-squares adjustment. $(SV/P)_z$ is a strongly nonlinear function of the fault parameters, so the solution found by the procedure is inherently nonunique. The acceptable solutions can be quite well constrained if the slip direction can be estimated initially on the basis of independent information.

A variety of tests of the procedure have been carried out on real and synthetic data. Given a set of amplitude data for an earthquake in Bear Valley, California, and told only that the mode of slip was predominantly strike-slip, the program "found" the San Andreas fault, i.e., converged to a fault with strike and dip close to the known values. Further work on a German earthquake served to bring out some of the ambiguities of the solutions. Analysis of data from a brief swarm of earthquakes in southwest Germany showed that the method yields useful mechanisms for small events and revealed a rotation of the focal mechanisms during the swarm. Processing of amplitudes from synthetic seismograms gave a fault plane close to the known input, but marked disagreement between the *SV* amplitudes on the synthetic seismograms and the amplitudes predicted by simple dislocation theory is unresolved.

INTRODUCTION

The principles underlying a method for determining the strike, dip, and slip direction of an earthquake mechanism from the distribution of the ratio of the amplitudes of S and P waves at distances less than about 100 km were established in a recent paper, referred to in the following as Paper I (Kisslinger, 1980). The usefulness of the method was demonstrated by several examples, and some of the pitfalls likely to be encountered in applying it were explained. Computational procedures for routine analysis of typical local network data have now been developed. The availability of these computer programs has made it possible not only to process data rapidly and more thoroughly than was done previously, but also to carry out a variety of numerical experiments with real and synthetic data which serve to bring out further the subtleties and difficulties inherent in the technique.

The goal of the analysis is to find a focal mechanism which yields calculated ratios of the vertical component of SV to the vertical component of P in satisfactory agreement with the observed values of this quantity. The basis of the computations and the advantages in using this particular quantity, designated as $(SV/P)_z$, as the observed datum are explained in Paper I.

The dependence of $(SV/P)_z$, on the fault parameters is strongly nonlinear and the

"best-fitting" mechanism to a set of amplitude ratio data is not necessarily a well-constrained solution for the earthquake if all three parameters are free to vary arbitrarily. Some aspects of the inherent nonuniqueness have been discussed by Jones and Minster (1980). However, the analysis is expedited by the imposition of some constraints on the starting solution on the basis of independent information. Some constraints are mandatory if a claim that the solution is correct for the event is to be made. In Paper I, the initial constraint was imposed by fixing the fault motion as either pure strike-slip or dip-slip. The decision is based on some combination of first-motion polarities and knowledge of the regional tectonics. This approach still appears to be a satisfactory way to get the best starting solution and to choose among alternatives that may come out of the processing.

Summary of the Theory

The starting point for the calculations is the expression for the ratio of SV to P amplitudes generated by a point shear dislocation in an infinite, homogeneous medium. From Paper I, this is

$$(SV/P)_0 = \left(\frac{V_p}{V_s}\right)^2 \cot i_h \cdot \left[2 - \frac{(\cot\delta - \tan\delta)\sin\lambda \tan i_h \sin A + 2\sin\lambda + \csc\delta \cos\lambda \tan i_h \cos A}{D}\right] \quad (1)$$

where

$$D = \cos\lambda \cos A \sin i_h[-\sin i_h \sin A \sec\delta + \cos i_h \csc\delta] + \sin\lambda \sin i_h \cos i_h \sin A(\cot\delta - \tan\delta) + \sin\lambda(\cos^2 i_h - \sin^2 i_h \sin^2 A).$$

and

δ = dip of the fault
λ = direction of slip, measured in the fault plane from the strike
A = azimuth to the station, measured from the strike of the fault
i_h = take-off angle of the ray to the station at the source
V_p, V_s = P- and S-wave velocities.

The effects of the various boundaries in the earth model on the ratio as observed at the surface must be considered. As explained in Paper I, one of several advantages of using the amplitude ratio rather than the absolute amplitudes is that for a wide range of velocity contrasts and angles of incidence, the ratio of the SV-to-P transmission coefficients is close to 1, so that the effects of internal boundaries can be neglected. The validity of this assumption must be checked for each velocity model and range of distances used. Tables and figures such as those published by McCamy *et al.* (1962) and Costain *et al.* (1963) are useful for this purpose.

The ratio of SV to P amplitudes in the interior must be converted to the ratio of the vertical amplitudes of these waves, as observed on the free surface. This is done by using equations derived by Gutenberg (1944). The factor by which $(SV/P)_0$ must be multiplied to obtain $(SV/P)_z$, for Poisson's ratio of 0.25, is shown in Figure 1. Three salient features are seen. For arrivals, incident nearly vertically, at less than 30°, this correction is substantial and must be used. For angles of incidence in the range from about 30° to 37°, near the critical angle for SV-to-P conversion by

reflection, the correction changes very rapidly with the angle of incidence. Data from stations within this range should be excluded from the analysis because the angle of incidence cannot be known with sufficient accuracy to make the required correction. Finally, for waves incident at between 37° and 80°, the factor is close to 1 and no great loss of accuracy results from neglecting the free surface effect.

The effects of inelastic attenuation on $(SV/P)_z$ are illustrated in Figure 2 for a vertical strike-slip fault at a depth of 6 km in a layered model. This model consists of a layer 2 km thick, in which the P-wave velocity is 4 km/sec, overlying a layer 13 km thick, with P-wave velocity 5.9 km/sec, both overlying a half-space with a velocity of 6.8 km/sec. If the dominant frequencies of the two body waves are the same, the effects are quite strong even at short distances, for frequencies typical of those seen with conventional microearthquake instrumentation. However, if the S

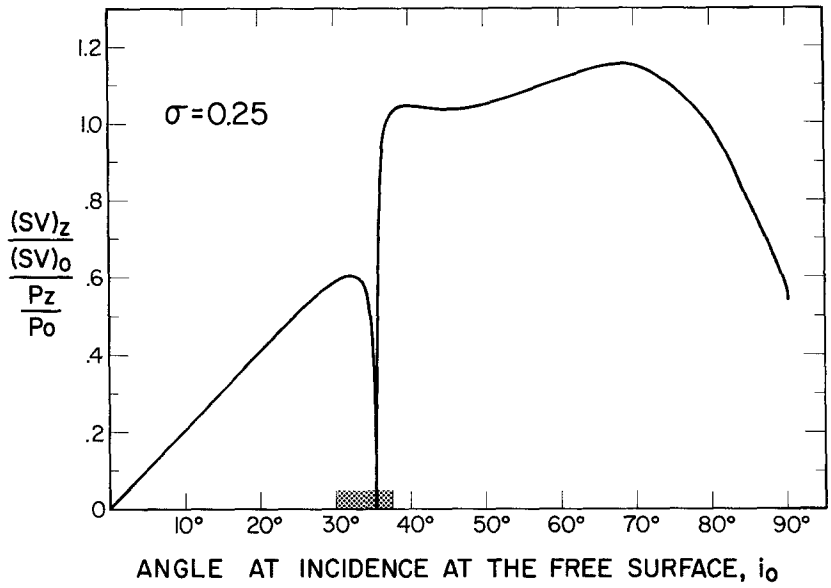

FIG. 1. Factor to convert the ratio of the amplitudes of incident SV to incident P into the ratio of the amplitudes of the vertical components. The *shaded* section, 30° to 37°, is the range of angles near the critical angle for SV-to-P conversion by reflection in which data should be rejected because of the difficulty in determining the surface factor (which also involves a large phase shift) with sufficient accuracy.

wave is characterized by a frequency somewhat lower than that of P, the efffects of the lower Q for S and the frequency offset in a way that makes the resulting change in $(SV/P)_z$ with distance hardly distinguishable from the case of perfect elasticity. As shown in Paper I, the Central California data seemed to fit the theoretical values for infinite Q well enough, but the full investigation of the effects of Q on the focal mechanisms obtained by this method has not yet been done.

THE PROCEDURE

The steps in the analysis are illustrated in block diagram form in Figure 3. The required input is the best available hypocenter solution for the earthquake and a set of observations of $(SV/P)_z$ at the N stations of the network. SV and P amplitudes are read as the maximum peak-to-peak amplitude within the first three half-cycles of the direct arrivals as recorded on the vertical component. Reference to a set of

travel-time curves appropriate for the velocity model and depth of focus is useful for checking whether stations are near cross-over points or triplication points for various ray paths, where the amplitudes are contaminated by interfering arrivals. The method has so far been limited mostly to the use of upward traveling direct waves to the stations, but there is no reason in theory that downward traveling waves that reach the station after refraction or reflection cannot be used, as long as the P and S amplitudes that are compared have traveled the same path. The azimuth to each station and the take-off angle of the direct ray are read from the hypocenter solution. The corresponding angle of incidence at the free surface and the free surface factor must be calculated to give $(SV/P)_z$ taken from a curve, as in Figure 1, or a table. Errors in the position of the hypocenter, especially depth errors, cause errors in the azimuth and take-off angle, which produce errors in the focal mechanism, just as they do for more conventional methods. Similarly, errors in the velocity model cause

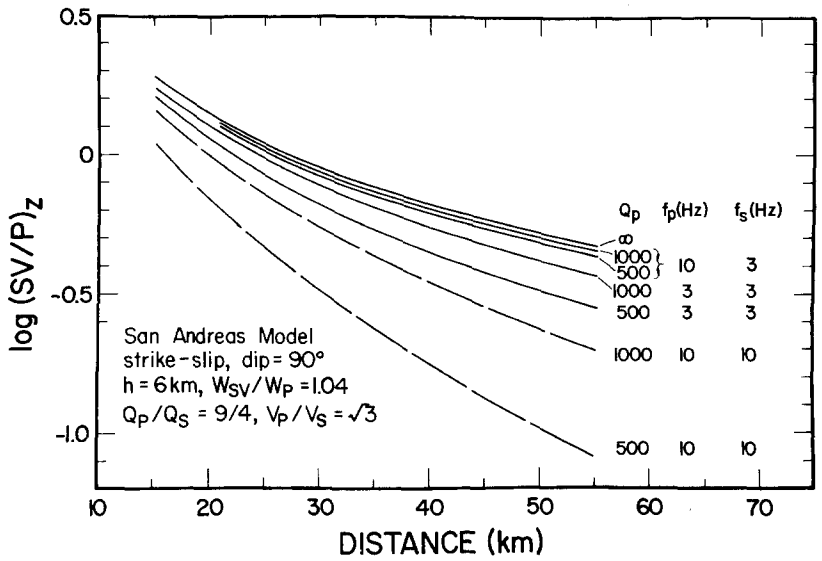

FIG. 2. The effects of finite Q on $(SV/P)_z$ for a vertical strike-slip fault. Note the possibility of offsetting effects of frequency and Q for the second and third curves from the top.

errors in the take-off angle and the angle of incidence at the surface, which affect the free surface correction.

There are two possible entries into the computational procedure. If there is sufficient independent information to support a likely focal mechanism, the slip of that mechanism can be used as a starting slip. This decision has a strong influence on the outcome of the analysis; the problem is so strongly nonlinear that the linear least-squares adjustment to be used subsequently cannot be relied on to compensate for a bad choice of the starting value of the slip direction. It is encouraging that in a number of cases where the evidence for a particular mode of faulting is very strong, the process would not converge when the wrong starting slip was intentionally used, so that no result, rather than a misleading one, was obtained. When there is insufficient information for choosing a starting slip, the program can be used to try as starting values all slip angles, 0° through 180°, in selected small steps, in order to identify all plausible starting solutions. These starting solutions are those

that have a fault dip with reasonably small scatter for some strike, for the given slip direction.

With the selected slip direction, the program then searches for the best-fitting solution, in the following sense. The basic theory [equation (1)] shows that for a given slip direction and assumed fault strike, there are, generally, two values of the dip of the fault that will yield the observed value of $(SV/P)_z$, whatever it is. For an arbitrary fault strike, the pair of dips that correspond to the observed value of the

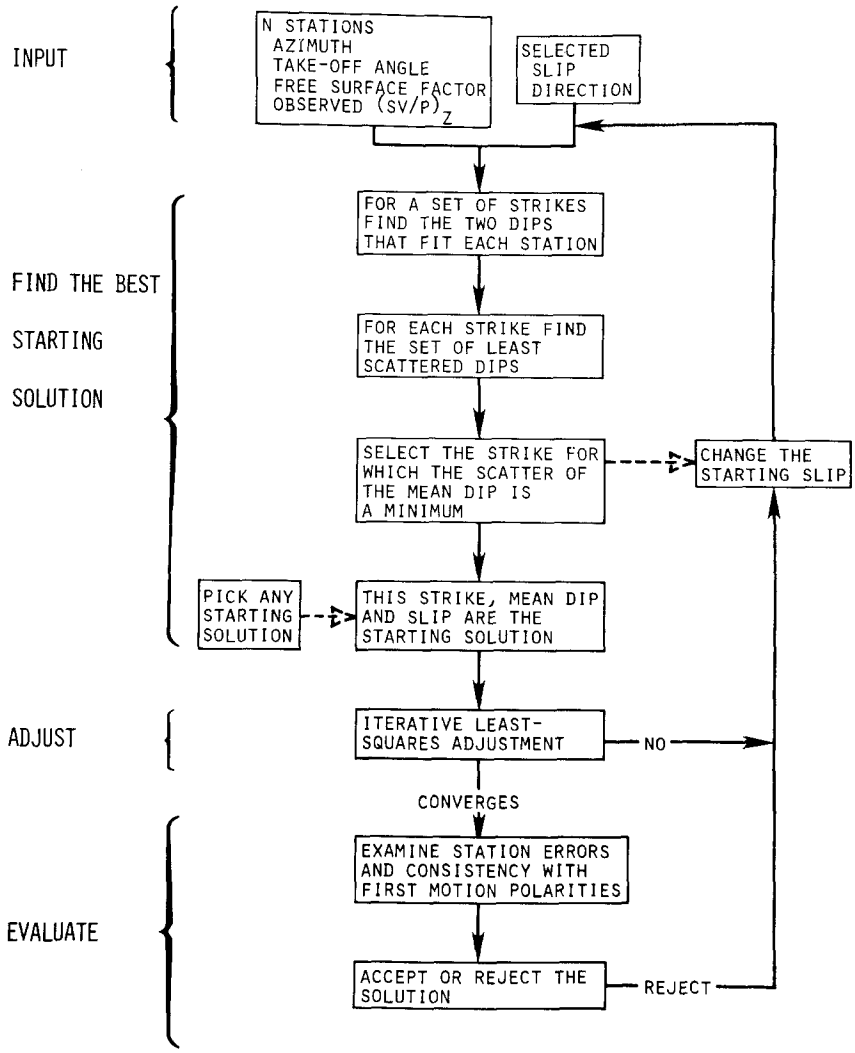

FIG. 3. Flow diagram for the computational procedure.

amplitude ratio for one station will be totally different from the pair that satisfy some other station. However, if the data are good, there must be some value(s) of the strike for which one of the two dip values for each station is close to one of the two for all of the other stations.

The first step in the process is to find the two values of dip for each station for each strike, with the values of strike incremented in selected small steps (10° in the standard program). Because of numerical difficulties which may occur, stations are

eliminated for the particular step in strike if the strike is the same as the station azimuth or, for the case of pure strike-slip, is 90° from the station azimuth.

In the search for the best starting solution, for pure strike-slip or pure dip-slip mechanisms only strikes from 0° to 180° need be tested, as the remaining values give redundant information. However, if some other slip value is used as the start, for example, the slip produced by the first computation, then all 360° must be searched.

The next step is to look through the array of strikes and $2N$-associated dip values for that strike for which one of the dips at each station is fairly close to one of the two values at all of the other stations. At this step it may be possible to identify and eliminate a station at which the amplitude data are bad, on the grounds that there is no strike value for which it yields a dip close to that of other stations. The N most clustered values of dip, one from each station, are selected, with the standard deviation of these values used as a measure of scatter. For some value of strike, the scatter of the best dips is the least. This strike and dip, with the selected slip direction, constitute the starting solution to which an iterative least-squares adjustment is applied. In many cases, a second strike-dip combination is present that is almost as good as the "best", i.e., the scatter of the dips is almost as small. This solution must also be examined. If no starting slip is given, the least-squares adjustment is applied to the two best strike-dip combinations corresponding to each possible slip direction.

The convergence criterion used is based on the sum squared errors of $\log(SV/P)_z$, which is a measure of the goodness of fit of the final solution. However, it is also necessary to check the calculated values at the individual stations against the observations (i.e., the residuals). Otherwise good-looking solutions which satisfy the convergence criterion can be eliminated if they leave large residuals for reliable observations. The basic lack of uniqueness in the method can be at least partially overcome in this way. The obvious last step is to check the solution against the available first motion data in order to avoid inconsistencies and also to resolve the basic inability of this method to give the sense of slip.

This procedure has been programmed for the PDP 11/70 at CIRES. One run, including the search for the best starting solution and the least-squares adjustment, takes about 2 min of CPU time for 6 to 10 stations. Sweeping through all possible slip directions in 2° increments and doing a least-squares adjustment for the two best starting solutions takes about 250 min of CPU time.

Tests of the Procedure

The procedure has been tested by more extensive processing of some of the earthquakes used in Paper I; application to some additional earthquakes and application to synthetic data. Because only the simplest computational and graphical techniques were used in Paper I, the slip directions were constrained to be either 0° or 90°. This severe restriction was removed and the effects of allowing arbitrary slip on the previous results examined.

Bear Valley event. The first test was done on a set of data from an earthquake with magnitude 1.3 that occurred in Bear Valley California on 9 April 1971, at a depth of 6.8 km. This event was selected as typical of small Bear Valley events analyzed in Paper I and because it had produced $(SV/P)_z$ data at 14 stations, ranging in distance from 10 to 57 km. The station at 10 km (EKH) was eliminated because the angle of incidence at the free surface, 36.4°, was too near the critical value (Figure 1). The important result of this test was that the program, with no

information other than the set of amplitude ratios and given a pure strike-slip start, found the San Andreas fault: fault strike = 130.46 ± 1.05°; fault dip = 87.37 ± 0.71°; slip direction = 0.99 ± 1.66°. The strike of the surface trace of the fault at the epicenter is about 138° and in Paper I the mean dip determined for that strike and pure strike slip was 89.5 ± 3.9°.

Another significant finding for this earthquake was that a test of all slip directions showed that only a strike-slip solution was acceptable. A slip angle as small as 4° led to a nonconvergent result, whereas 0° and 2°, converged to the solution given above. Because we are quite confident that we know the focal mechanism for earthquakes on this fault, this result is especially comforting.

The solution for this earthquake comes closer to justifying a claim of uniqueness than any other event tested. This may be because it is also the event with the largest number of stations. Because the deployment of instruments in the USGS, Central California network places many stations close to the fault trace, a large number of the data points may come from places near the nodal line in the direction of the fault. To test whether this particular station distribution might be the reason for the apparently excellent result, another determination was made on the basis of a reduced data set from which all stations (4) with azimuths from the epicenter within 10° of the strike of the surface trace of the fault were deleted. The solution generated was: fault strike = 136.82 ± 12.08°; dip = 88.80 ± 0.91°; slip direction = 0.40 ± 2.18°, still in good agreement with the known geology. Although the standard error of the strike is very large for this solution, the quality of the result as measured by the summed squared errors of $\log(SV/P)_z$ is better than for the solution with the full data set. This may be in part because the amplitudes at stations for which propagation is along the fault are distorted by either lateral velocity variations or fault-related differences in inelastic attenuation.

A less encouraging result is the discovery that if starting strikes and dips only slightly removed (≈10°) from the best start found by the program are inserted arbitrarily, the process will converge to significantly different results. The existence of many local minima within the whole parameter space is confirmed by this, as is the dominant effect of the starting solution on the result obtained.

Darmstadt event. The magnitude 2.3 earthquake of 7 June 1979 near Darmstadt, Germany, also analyzed in Paper I, was subjected to a detailed reexamination using the computational procedure described here.

The systematic scan of all slip directions yielded seven acceptable solutions (sufficiently small scatter of the starting mean dip and the least-squares adjustment converged). The search yields many more than seven slip directions with small scatter of the dip, but these converge by groups into one of the seven solutions. Two of the seven were almost pure dip-slip, and five, primarily strike slip. The first-motion polarities were well distributed in azimuth and ruled out all of the strike-slip solutions. The two dip-slip solutions were similar in strike, but differed in dip and slip direction: the conjugate pair for each solution are

Solution 1: $\text{strike}_1 = 131.80°$; $\text{dip}_1 = 45.29°$; $\text{slip}_1 = 87.90°$
$\text{strike}_2 = 308.81°$; $\text{dip}_2 = 44.75°$; $\text{slip}_2 = 92.13°$
Solution 2: $\text{strike}_1 = 129.94°$; $\text{dip}_1 = 36.99°$; $\text{slip}_1 = 98.81°$
$\text{strike}_2 = 320.91°$; $\text{dip}_2 = 53.52°$; $\text{slip}_2 = 83.42°$.

The subscripts "1" and "2" within each solution refer to the two conjugate fault planes. The method cannot distinguish between normal and reverse faulting, but

the first motions show this fault to be normal. The solution for this earthquake published in Paper I, based on the assumption of pure dip slip, was 313°, 45.4°, or solution 1 above. The two solutions found are almost indistinguishable in terms of all three parameters, but all of the measures of goodness of fit, mean error, summed squared errors, and standard errors of the three solution parameters all indicate that solution 2 is slightly better.

Although the significance is not clear, it is worth noting that all seven of the solutions that emerged, strike- and dip-slip alike, each had one fault plane with a southeast-northwest dip, all but one dipping to the southwest. Whether a common feature of this kind is typical of the multiple solutions emerging from this procedure is not yet known, but the possibility of a trade-off between dip and slip direction for strikes within a fairly narrow band seems real.

Freiburg sequence. On 12 June 1972, a sequence of six small earthquakes magnitudes 1.6 to 1.9 occurred between 00:30 and 06:22 UTC, within 1 to 2 km of 48°01'N7°55'E, in a depth range from 15.8 to 17.6 km, as determined by the Geophysical Institute, University of Karlsruhe. On 14 June one more very small event was located at almost the same place, just east of Freiburg, Baden-Wuerttemberg, southwest Germany. A striking feature of the sequence is illustrated by the seismograms in Figure 4. A clear change in $(SV/P)_z$ for the sixth event compared to the first is seen at station FEL, with the change at SCH almost as certain. The amplitude ratio at BUH is not significantly different. These two earthquakes were located as being within 1 km of each other. A change in the orientation of the fault plane of event 6 compared to event 1 seems to be demanded by this observation.

Events 1, 2, 3, and 6 were analyzed by means of the technique of this paper. Amplitude ratios at only four or five stations well distributed in azimuth were available as input. Events 4 and 5 occurred only about 1 sec apart, so their amplitudes could not be untangled. Event 7 was too small to use. All of the solutions are almost pure strike-slip on steeply dipping faults. It should be noted that the sparse first-motion polarities were added to the solution diagrams after the solutions were determined from amplitudes alone. In all cases, the first motions are consistent with the amplitude-ratio solutions. The slip angles given are consistent with the sense of motion required by the first motions. Events 1, 2, and 3 yielded almost identical solutions, with the mean values of the parameters approximately as follows

$$\text{strike}_1 = 38°;\quad \text{dip}_1 = 81°;\ \text{slip}_1 = -1°$$
$$\text{strike}_2 = 308°;\ \text{dip}_2 = 89°;\ \text{slip}_2 = 171°.$$

The solution for event 1 is illustrated in Figure 4.

The solution for event 6, also shown on Figure 4, is

$$\text{strike}_1 = 339°;\ \text{dip}_1 = 84°;\ \text{slip}_1 = -17°$$
$$\text{strike}_2 = 70°;\quad \text{dip}_2 = 73°;\ \text{slip}_2 = 186°.$$

The subscript "1" refers to the left-lateral fault, "2" to the right-lateral fault in each case, on the assumption that the sense of slip did not change as the fault plane rotated. The conclusion is that the fault plane rotated counterclockwise through about 58° between the first three and the sixth event in this brief sequence. Although the seventh event, 2 days later, was too small to permit analysis, the seismogram at station FEL, with a large P wave relative to S, suggests clearly that the focal mechanism is similar to that of event 6.

As a test, solutions for three of these earthquakes were sought starting from a pure dip-slip. The adjustment for event 1 diverged rapidly. For events 2 and 3 the process quickly moved to a strike-slip motion and slowly converged to solutions very similar to those found from a strike-slip start. This result was very encouraging.

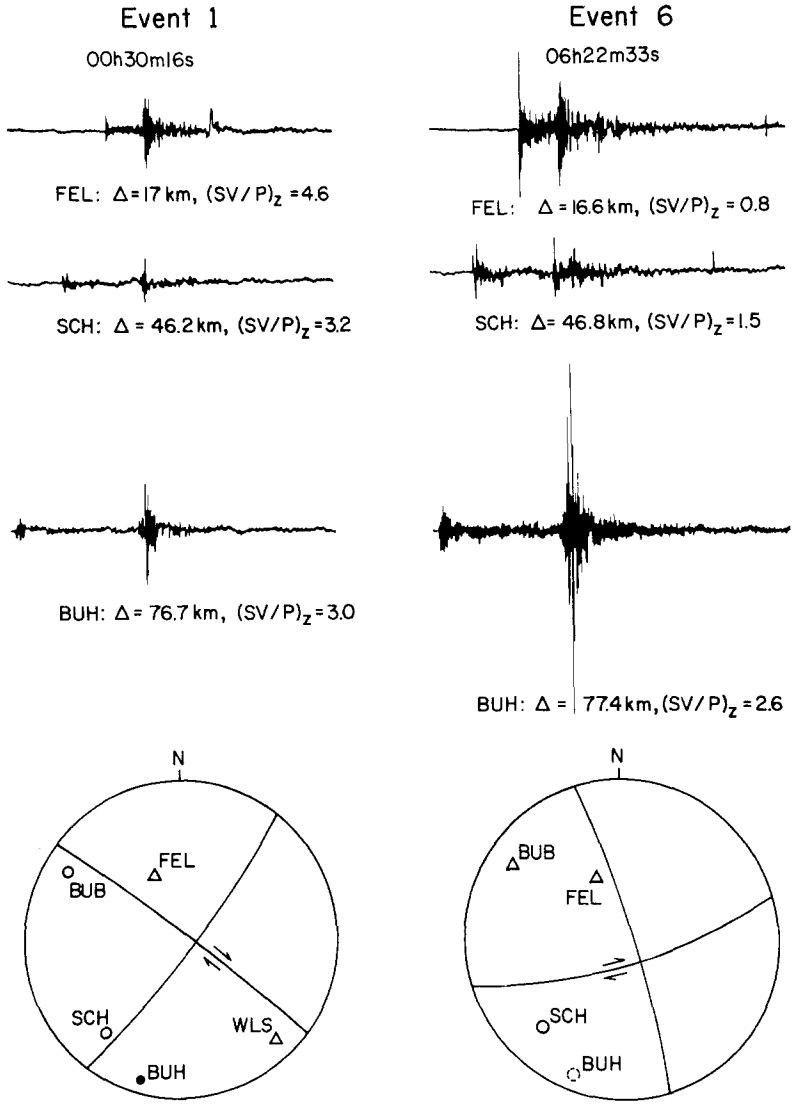

FIG. 4. Vertical component seismograms and focal mechanisms for two events in the Freiburg sequence. The records at FEL show the remarkable change in $(SV/P)_z$ for two earthquakes 6 hr apart at almost the same place. The first-motion polarities (circles for compression, triangles for dilatation, dot for uncertain) were added after the focal mechanisms had been calculated from the amplitude data.

This analysis shows that even with few data, if these are of good quality and well distributed in azimuth, this procedure will produce useful fault plane solutions for small earthquakes. In addition, the geophysically interesting result is that a pronounced change in fault plane strike can occur in a very limited volume within a short time.

Synthetic data. Values of $(SV/P)_z$ calculated from equation (1) have been used as input data to the program to test the internal consistency of the procedure. The fact that the procedure gives back the known input source, with zero error for the computed values of the three fault parameters, only demonstrates that the program is doing what it is supposed to. Tests of this kind were useful, however, not only for debugging the program, but also for testing the effectiveness of the algorithms used. For example, three methods of selecting one value of dip from the two found for each station for a given strike were tried. The desired result is a selection of one dip for each station such that the standard deviation about the mean of the N values is a minimum. The method adopted starts with a calculation of the mean of the $2N$ values and finds the single value at any station farthest from that mean. That extreme value is replaced by the other value for that station and the "better" value for that station is then fixed. The process is repeated until a value is chosen for each station. The mean and standard deviation are then calculated and filed. If the two values for a station are both very far from the final mean value, the method may pick the value farther from the final mean, so it has erred. However, in all such cases the "best-fitting" dip is so badly scattered that it and the strike that goes with it would not be considered as reasonable starting values, so the failure of the algorithm in these extreme cases does not lead to any error in the final result.

Tests on synthetic seismograms have yielded more ambiguous results. Synthetic seismograms for vertical strike-slip and 45° dip-slip faults, for distances typical of those used in the real earthquakes and for representative azimuths were calculated by M. Knecht of the Geophysical Institute, Karlsruhe using the program for the reflectivity method as developed by R. Kind (1978). Seismograms for some of the same cases were also calculated by D. Harvey of CIRES with his mode superposition program. The results of the two techniques were essentially indistinguishable.

The reflectivity calculations were carried out for $Q_\alpha = 1000$, $Q_\beta = 444$, dominant signal frequency of 3.2 Hz and a velocity model simulating the upper crust along the San Andreas fault in central California. The most thorough study was done for the case of the 45°-dipping, dip-slip fault, at a depth of 6 km. The greatest difficulty was finding the S wave on the synthetic seismograms. Beyond 15 or 20 km, the S amplitudes were much smaller relative to P than predicted by the dislocation theory. At some distances this was clearly due to interference of other arrivals, but the discrepancies are not yet understood. It was found that the agreement at all distances and azimuths was much better if the "data", i.e., synthetic seismogram amplitudes, were corrected for Q_α, Q_β of 250, 111, respectively, instead of the values known to have gone into the calculations.

In spite of this disagreement of the synthesized $(SV/P)_z$, the fault mechanism obtained from the analysis was in satisfactory agreement with the known input when the "data", corrected for Q were used. The raw data, not Q-corrected, yielded a solution in poor agreement, strike = 308°, dip = 44.9°, slip = 110.8°, compared to the correct values of 360°, 45°, 90°. The data corrected for the known Q's gave a much better result: 355.9; 41.6; 91.2, with smaller standard errors on all three parameters. The fact that the synthetic amplitudes gave back the known input source mechanism when the correction for Q was made and not otherwise is taken as evidence that the overall procedure is basically correct.

The synthesized P arrivals agree with the radiation pattern predicted by the dislocation model, for both strike-slip and dip-slip faults. The relative amplitudes of the P arrivals as a function of distance and azimuth for the two modes of slip are as expected. The problem appears to be with the S waves. It is very likely that the

smaller than expected S waves are the result of interference with multiply reflected waves in the low-velocity surface layer. Further tests with different models are planned to try to resolve the apparent discrepancy.

The need for a correction for finite Q to get a good result for the synthetics, while, for example, the data for Bear Valley, California, are well fit by the infinite Q theory, probably arises because the frequency of both body waves is fixed at the same value in the synthetic seismograms, while a compensating lower frequency may dominate for the S waves in the real case (see Paper I and Figure 2).

Conclusions

A convenient computational procedure has been developed for deriving the strikes, dip, and slip direction of a fault from observations of $(SV/P)_z$ at short epicentral distances. A variety of tests demonstrate the validity of the approach and show that useful focal mechanism solutions can be obtained from sparse data, especially if the basic mode of slip is known independently. Solutions can be based on data from as few as four stations, but five or six seem to be the minimum for which a reasonably well-constrained solution will result. The distribution of the stations is as important as the number, as some stations must be at azimuths for which the amplitude ratio is either high or low if the strike of the fault is to be resolved with acceptable precision. There is a wide range of strikes for any mechanism for which the amplitude ratio at a given station is almost constant.

This disagreement between values of $(SV/P)_z$ calculated by the method of this paper and those taken from synthetic seismograms is not resolved. Further tests, using a variety of velocity models will be done to try to find the source of the apparent conflict. It is encouraging that in spite of this disagreement, the focal mechanism obtained from the synthetic data is close to the known input.

Acknowledgments

The principal support for this research was provided by the U.S. Geological Survey, through Contract 14-08-0001-19272. The work was initiated while one of the authors (C. K.) was a guest of the Geophysical Institute, University of Karlsruhe, Federal Republic of Germany, under an award from the Alexander von Humboldt Foundation. We thank Klaus-Peter Bonjer of Karlsruhe for bringing the Freiburg sequence to our attention and for providing the seismograms and hypocenter locations for those events. Steve Ihnen was very helpful in the initial modification of the programs for use on the CIRES computer.

References

Costain, J. K., K. L. Cook, and S. T. Algermissen (1963). Amplitude, energy, and phase angles of plane *SV* waves and their application to earth crustal studies, *Bull. Seism. Soc. Am.* **53,** 1039–1074.

Gutenberg, B. (1944). Energy ratio of reflected and refracted seismic waves, *Bull. Seism. Soc. Am.* **34,** 85–101.

Jones, C. and B. Minster (1980). Local earthquake focal solutions using *P-SV* amplitude information (abstract), *EOS* **61,** 1028.

Kind, R. (1978). The reflectivity method for a buried source, *J. Geophys.* **44,** 603–612.

Kisslinger, C. (1980). Evaluation of S to P amplitude ratios for determining focal mechanisms from regional network observations, *Bull. Seism. Soc. Am.* **70,** 999–1014.

McCamy, K., R. Meyer, and T. J. Smith (1962). Generally applicable solutions of Zoeppertz's amplitude equations, *Bull. Seism. Soc. Am.* **52,** 923–955.

Cooperative Institute for Research in
Environmental Sciences
Department of Geological Science
University of Colorado
Boulder, Colorado 80309 (C.K., J.R.B.)

Geophysical Institute
University of Karlsruhe
D-7500 Karlsruhe
Federal Republic of Germany (K.K.)

Manuscript received May 19, 1981